Macromolecules

pubs.acs.org/Macromolecules Article

Synthesis of Bifunctional Copolyesters via Chemoselective Ring-Opening Copolymerization of δ-Lactone Derived from CO_2 and Butadiene with ε-Caprolactone

Junhao Shen,[§] Jinbo Zhang,[§] Wenhui Kong, Yuanchi Ma, Shaofeng Liu,* and Zhibo Li*

Cite This: *Macromolecules* 2025, 58, 3497−3508 Read Online

ACCESS | Metrics & More | Article Recommendations | Supporting Information

ABSTRACT: 3-Ethylidene-6-vinyltetrahydro-2*H*-pyran-2-one (EVP), derived from the telomerization of carbon dioxide (CO_2) with 1,3-butadiene, emerges as a promising intermediate for the production of high-value added materials from CO_2. However, the current impediment lies in the challenge of accessing selective ring-opening (co)polymerization of EVP because of unfavorable thermodynamics under mild conditions and the competitive polymerization of highly reactive C═C double bonds. In this study, we report the chemoselective ring-opening copolymerization of EVP (selective ring-opening rather than vinyl polymerization) with ε-caprolactone (CL), even at room temperature, by using a phosphazene/urea binary catalyst. This process exclusively yields the ring-opening product of copolyester poly(CL-*co*-EVP). The resultant poly(CL-*co*-EVP)s exhibit predictable molar masses (M_ns), narrow distributions ($Đ$ < 1.2 for most cases), wide range of EVP-contents (0−60 mol %), and thus tunable thermal properties. The kinetic and reactivity ratio (r_{CL} = 3.67 and r_{EVP} = 0.17) studies indicate a gradient structure for poly(CL-*co*-EVP). Moreover, these poly(CL-*co*-EVP)s possess two distinct pendant alkene groups, an internal one and a terminal one, which are ready to undergo sequential functionalization to prepare bifunctional polyesters or form cross-linked polyesters. Poly(CL-*co*-EVP) copolyester with only a 2 mol % EVP incorporation shows a significant improvement in both tensile strength (σ_b) and elongation at break (ε_b) in comparison to PCL homopolymer with a similar M_n, while cross-linking further facilitates the transformation of PCL from thermoplastics to elastomers. This study opens avenues to utilize EVP and synthesize sustainable and functional polyesters.

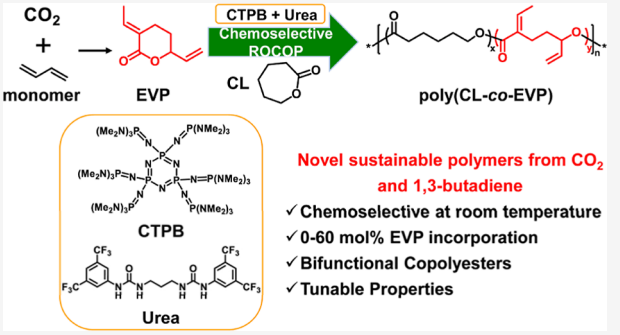

1. INTRODUCTION

The application of 3-ethylidene-6-vinyltetrahydro-2*H*-pyran-2-one (EVP), synthesized through the telomerization of 1,3-butadiene with CO_2 (Scheme 1A),[1−8] represents a highly impactful strategy to develop sustainable polymers.[9−14] The cost-effectiveness and abundant availability of 1,3-butadiene and CO_2 further contribute to its appeal.[15−19] Consequently, it has received significant attention for long-term sustainability for the synthesis of high CO_2-content polymers. It is noteworthy that EVP possesses two pendant alkene groups capable of undergoing radical, coordination, and conjugate addition polymerization.[9−13] In 1998, Dinjus pioneered the polymerization of EVP through "thiol−ene" click copolymerization with dithiols, yielding copolymers with the cyclic lactone incorporated into the polymer backbone.[20] In 2014, Nozaki and co-workers achieved a significant progress to synthesize polyacrylates by free-radical polymerization of EVP.[21] The same group further discovered that EVP can undergo coordination/insertion copolymerization with alkene, catalyzed by Pd complexes, yielding polyolefins appended with lactone functionalities.[22,23] Recently, Lin and co-workers reported O_2-initiated radical polymerization of EVP to synthesize CO_2-derived polymers with high molar masses.[24]

In order to synthesize EVP-derived polyesters, Eagan and co-workers reported the polymerization of EVP via divergent propagation mechanisms, combining 1,4-conjugate addition and ring-opening polymerization reactions.[25] On the other hand, Tonks[26,27] and Lin[28,29] reported the synthesis and ROP of two derivatives of EVP: α-ethyl-δ-vinyl-δ-valerolactone (EtVP) and 3,6-diethyl-tetrahydro-2*H*-pyran-2-one (DEP), wherein the unsaturated C═C double bonds were partially (former) or completely (latter) hydrogenated. Recent studies demonstrated the synthesis of linear unsaturated poly-$(EVP)_{ROP}$ polyester via chemoselective ring-opening homopolymerization of EVP using phosphazene/urea binary catalysts.[30,31] Nevertheless, the conversion of EVP was limited

Received: January 8, 2025
Revised: March 11, 2025
Accepted: March 18, 2025
Published: March 27, 2025

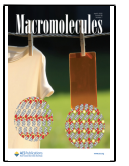

Scheme 1. (A) Synthesis and (B–D) Ring-Opening Copolymerization (ROCOP) of EVP with Other Lactones

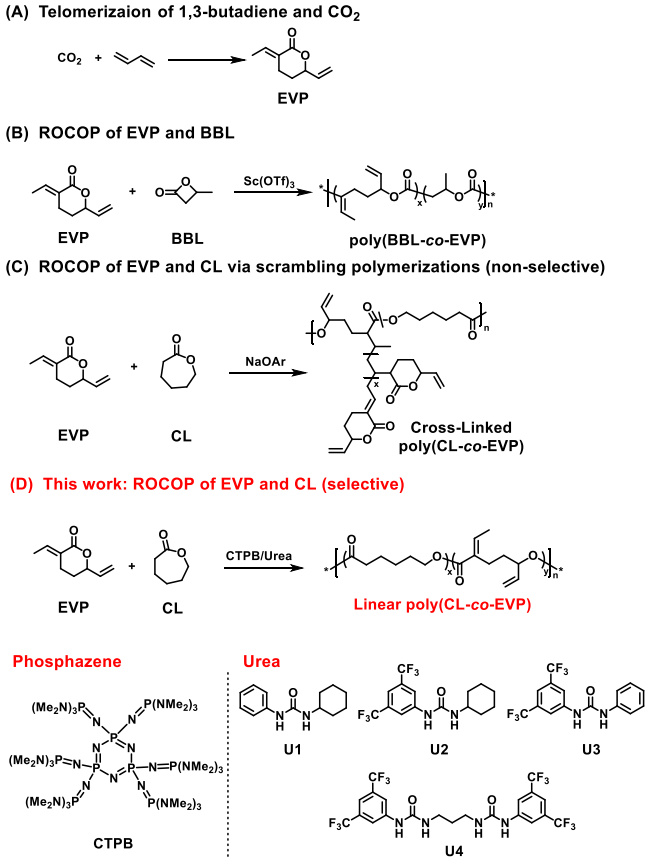

to ∼30% at −50 °C and the resulting polymer had relatively low M_n, due to unfavorable thermodynamics toward its ROP.[14,32,33]

Another strategy for ROP of a cyclic monomer with low strain and activity is ROCOP with a highly strained and active comonomer because the introduction of a second monomer would increase the entropy (ΔS) and decrease the Gibbs free energy (ΔG) of polymerization system.[34−37] Moreover, copolymerization has been proven as a powerful method to synthesize polymers with customized properties through regulating both composition and sequence distribution of the resulting copolymers.[38−43] In 2021, Ni and co-workers successfully reported ROCOP of EVP with β-butyrolactone (BBL) using $Sc(OTf)_3$ (Scheme 1B).[44] However, the resulting copolymer had a low molecular weight (M_w) of 4.1 kDa and a broad dispersity of 3.66 due to unavoidable chain transfer of cationic propagating chain ends. The same group further employed $Sc(OTf)_3$ to catalyze the cationic ROCOP of EVP with CHO or PO, producing a random polyester-*co*-polyether with the M_n of 6.5 kDa and $Đ$ of 2.2.[45] In addition, they also developed "scrambling polymerizations" of EVP with CL and synthesized cross-linked poly(CL-*co*-EVP) polyesters (Scheme 1C).[46] Recently, Tang and co-workers utilized a chromium salen complex as the catalyst to copolymerize EVP with epoxides for the synthesis of functional and degradable polyester-*co*-polyethers, involving in situ generation of the EVP-dimer through Cr-catalyzed 1,4-vinylogous Michael addition.[47] Hence, the ROCOP of EVP with other lactones to synthesize well-defined copolyesters is conceptually appealing but very challenging, and finding catalytic systems that can precisely control ROP of EVP while avoiding side reactions is crucial.

Table 1. ROCOP of EVP and CL Catalyzed by CTPB/Urea Under Different Reaction Conditions[a]

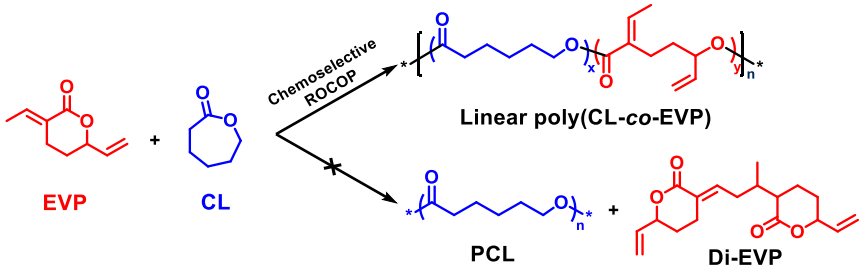

run	urea	CTPB/urea	[M] (M)	temp. (°C)	conv.[b] (EVP, %)	conv.[b] (CL, %)	select.[c] (%)	incorp.[b] (mol %)	$M_{n,theo.}$[d] (kDa)	$M_{n,NMR.}$[e] (kDa)	$M_{n,SEC}$[f] (kDa)	$Đ$[f]
1	U1	1/2	1.6	−25	33	95	40	10			16.5	1.57
2	U2	1/2	1.6	−25	16	96	100	14	6.7	6.0	10.3	1.11
3	U3	1/2	1.6	−25	21	99	100	18	7.2	6.6	9.4	1.13
4	U4	1/1	1.6	−25	32	99	100	24	8.1	7.2	10.0	1.31
5	U4	1/1	1.6	−60	38	72	100	35	7.0	6.6	11.0	1.08
6	U4	1/1	1.6	−50	38	99	100	28	8.5	8.0	10.8	1.19
7	U4	1/1	1.6	0	15	99	100	13	6.8	6.2	7.2	1.49
8	U4	1/1	1.6	25	11	99	100	10	6.5	6.3	9.0	1.44
9	U4	1/1	1	−50	30	96	100	24	7.8	7.4	9.1	1.11
10	U4	1/1	3	−50	53	99	100	35	9.7	8.6	10.3	1.19
11	U4	1/1	4	−50	55	96	100	36	9.7	8.5	13.7	1.16

[a]Conditions: CTPB (0.02 mmol, 24 mg), 8 h, EVP/CL/BDM = 50/50/1, [M] = $[EVP]_0$ + $[CL]_0$, THF was used as solvent. [b]Determined by ^1H NMR spectroscopy. [c]EVP polymerization selectivity via ROP pathway determined by ^1H NMR spectroscopy. [d]$M_{n,theo.}$ = $[EVP]_0/[I]$ × conv.(EVP) × M_{EVP} + $[CL]_0/[I]$ × conv.(CL) × M_{CL} + M_{BDM}. [e]$M_{n,NMR.}$ = Integration (6.95 to 6.80 ppm) × M_{EVP} + Integration/2 (4.15 to 4.00 ppm) × M_{CL} + M_{BDM}. [f]Determined by size exclusion chromatography (SEC) in THF at 40 °C relative to PS standards.

https://doi.org/10.1021/acs.macromol.5c00076
Macromolecules 2025, 58, 3497−3508

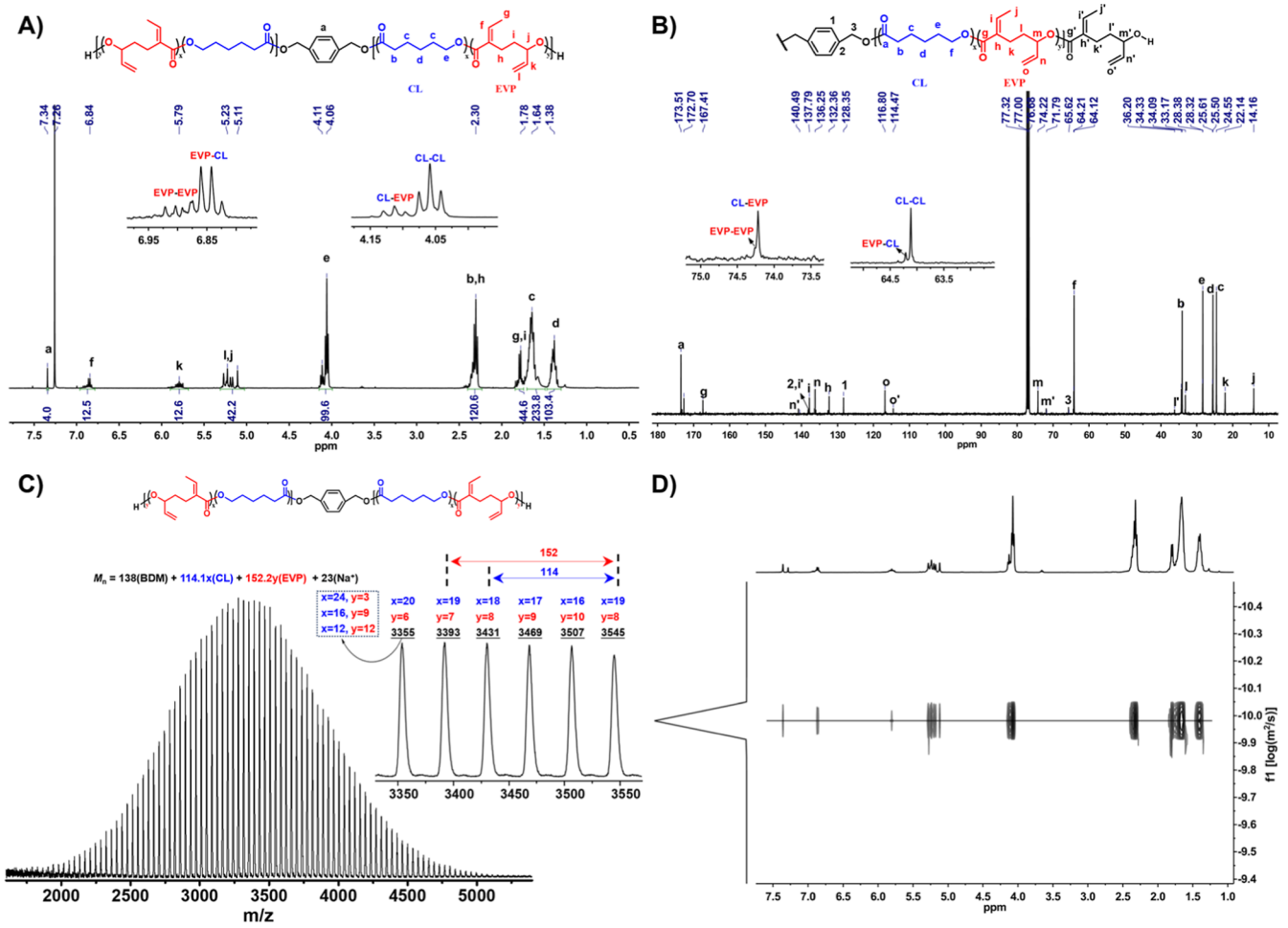

Figure 1. (A) ^{1}H NMR, (B) ^{13}C NMR, (C) MALDI-TOF mass spectrum, and (D) DOSY NMR of poly(CL-*co*-EVP) copolyester with a 28 mol % EVP incorporation (Table 1, run 6).

In this contribution, we report that the controlled and chemoselective ROCOPs of EVP with CL are achieved, even at room temperature, by using a phosphazene/urea binary catalyst (Scheme 1D). The resulting well-defined poly(CL-*co*-EVP)s have controlled molar masses, narrow distributions ($Đ$ < 1.2 for most cases), wide range of EVP-contents (0−60 mol %), and thus tunable thermal properties. Notably, these copolyesters contain two distinct pendent C═C double bonds and thus can be properly functionalized by Michael addition reaction and photoinduced thiol−ene click reaction to synthesize bifunctional polyesters.

2. RESULTS AND DISCUSSION

Recently, we reported chemoselective ROP of EVP for the first time and synthesized polyester poly(EVP)$_{ROP}$ exclusively, using base/urea (Scheme 1D) as the binary catalytic system.[30] It was found that CTPB with optimal basicity and molecular size, in combination with various ureas, was superior in the chemoselective ring-opening homopolymerization of EVP, as compared to *t*-BuP$_2$ and *t*-BuP$_4$. Inspired by these findings, CTPB with various ureas was employed for further investigation on the chemoselective ROCOP of EVP and CL in this study. Thus, four ureas containing different substituents were employed together with CTPB as binary catalysts for the ROCOP of EVP and CL, and the results are detailed in Table 1. The ROCOPs of EVP and CL were initially explored at −25 °C in THF utilizing BDM as the initiator, with a feeding molar ratio of EVP/CL = 1/1 and a total monomer concentration of 1.6 M (Table 1, runs 1−4).

Crude mixtures were subjected to ^{1}H NMR analysis to monitor the conversions of EVP and CL, as well as the formations of poly(CL-*co*-EVP) and other byproducts (Supporting Information Figure S1). For comparison, CTPB without urea was also tested as a single catalyst under otherwise identical conditions, producing a mixture of dimer (Di-EVP) and poly(CL-*co*-EVP) copolyester with a chemoselectivity of 24% through the ROP pathway (Table S1, run 1), as confirmed by the resonances at 7.05 and 6.86 ppm in the ^{1}H NMR spectrum (Figure S1). When U1 was used, the chemoselectivity increased to 40%. The introduction of a 3,5-bis(trifluoromethyl) phenyl group (U2 and U3) led to a dramatically increasing chemoselectivity from 40% to 100% through the ROP pathway (Table 1, runs 2 and 3). Intriguingly, a bis-urea (U4) was employed to show both high catalytic activity and 100% chemoselectivity toward the ROCOP of EVP and CL (Table 1, run 4). The copolymerization reached an EVP conversion of 32% and a CL conversion of 99% within 8 h, yielding a copolyester with an EVP incorporation of 24 mol % (Figure S 1d). It has been reported that the bis-urea in a base/urea catalytic system usually displays better activity than monourea under otherwise identical conditions.[48] Similar phenomenon was observed in

https://doi.org/10.1021/acs.macromol.5c00076
Macromolecules 2025, 58, 3497−3508

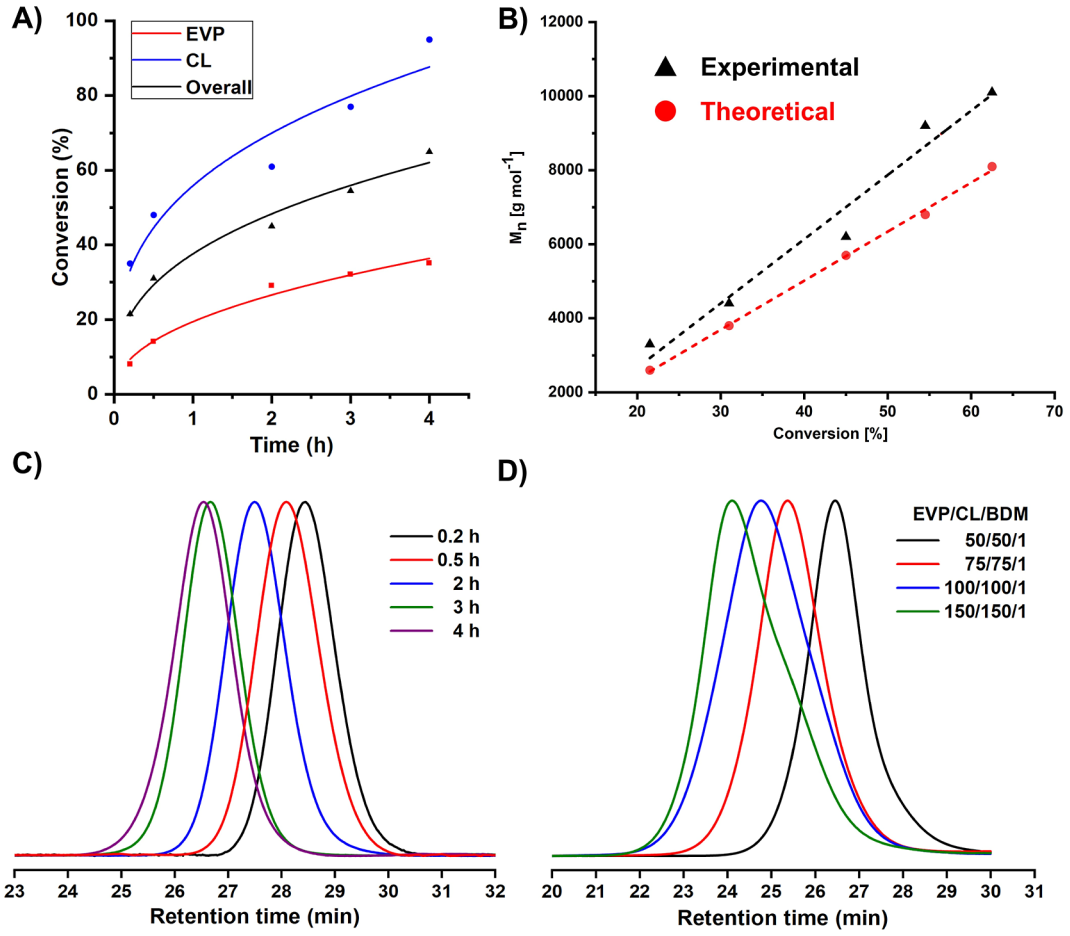

Figure 2. (A) Kinetic profiles of EVP (red square) and CL (blue circles) monomer conversions. (B) M_ns of resulting copolyesters with different overall monomer conversions. SEC traces of poly(CL-*co*-EVP) (C) at different overall monomer conversions (data shown in Table S1, runs 3−7) and (D) at various ratios of EVP/CL/BDM (data shown in Table 1, run 6 and Table 2, runs 1−3).

our recent report on ring-opening homopolymerization of EVP.[30] Therefore, the catalyst (urea and CTPB) is crucial for achieving chemoselective ROCOP of EVP and CL. Based on these results, bis-urea U4 was selected to construct binary organocatalyst in combination with CTPB for further ROCOP tests, and the results are shown in Table 1, runs 4−11.

The temperature was also identified as a crucial factor in the chemoselective ROCOP of EVP with CL. Consequently, ROCOP reactions were carried out over a temperature range from −60 to 25 °C (Table 1, runs 4−8; Figure S2). It was remarkable that all copolymerizations were 100% selective toward ROCOPs of EVP and CL, even at 25 °C (Figure S2e). These results are quite unexpected because only nonselective ROPs of EVP were obtained at 25 °C in previous reports.[25,30] Thus, the strategy of copolymerizing with a second monomer for conventional ROP of EVP under mild conditions is successful in this study, although the conversion of EVP was still relatively low at 25 °C (Table 1, run 8). At −50 °C, the EVP conversion increased to 38%, producing the desired poly(CL-*co*-EVP) copolyester with 28 mol % EVP incorporation (Table 1, run 6). These results indicate that the low polymerization temperature provides additional thermodynamic control to further enhance the conversion of EVP. Further decreasing the temperature to −60 °C resulted in a 72% conversion of CL within 8 h (Table 1, run 5) and a 89% conversion of CL within 12 h (Table S1, run 2), probably due to the diminishing solubility of urea at such a low temperature.[49] However, a poly(CL-*co*-EVP) copolyester with a high EVP incorporation up to 35 mol %, a $M_{n,SEC}$ of 11.0 kDa and a narrow distribution ($Đ$ = 1.08; Figure S3) was successfully synthesized. Note that the $M_{n,SEC}$ (11.0 kDa) exhibits a significant discrepancy compared with the theoretical value (7.0 kDa). To address this unexpected observation, the molar masses for resultant copolyesters were further measured by ^{1}H NMR spectroscopy, showing better agreement with theoretical ones (6.6 kDa vs 7.0 kDa).

Subsequent ROCOP of EVP with CL was carried out under varying initial monomer concentrations to enhance monomer conversion and the corresponding incorporation of EVP in poly(CL-*co*-EVP). Elevating the total monomer concentration to 3 M, an EVP conversion of 53% and an EVP incorporation of 35 mol % were obtained (Table 1, run 10), which was remarkable in comparison to the conversion of ∼30% for homopolymerization.[30] However, further elevating the monomer concentration to 4 M led to only a negligible increase in EVP conversion and incorporation (Table 1, run 11), probably due to the increasing viscosity preventing further polymerization (Figure S4).

2.1. Characterization of Poly(EVP-*co*-CL) Copolyesters. The obtained poly(CL-*co*-EVP) samples were carefully analyzed by 1D (^{1}H and ^{13}C) and 2D (heteronuclear single-quantum coherence (HSQC) and heteronuclear multiple bond correlation (HMBC)) NMR spectroscopy (Figures 1, S5 and S6), which offer detailed insights into the chain structures of

https://doi.org/10.1021/acs.macromol.5c00076
Macromolecules 2025, 58, 3497−3508

Table 2. ROCOP of EVP and CL with Different Feeding Ratios by CTPB/U4[a]

run	EVP/CL/BDM	conv.[b] (EVP, %)	conv.[b] (CL, %)	select.[c] (%)	incorp.[b] (%)	$M_{n,theo}$[d] (kDa)	$M_{n,NMR}$[e] (kDa)	$M_{n,SEC}$[f] (kDa)	$Đ$[f]
1[g]	75/75/1	41	99	100	29	13.1	10.3	15.8	1.16
2[g]	100/100/1	40	98	100	29	14.9	12.7	19.4	1.23
3[g]	150/150/1	37	97	100	28	25.0	19.5	22.6	1.24
4	0/100/1		>99		0	11.4	10.7	21.6	1.59
5	10/90/1	40	83	100	5	7.8	7.8	9.7	1.40
6	20/80/1	44	90	100	11	8.5	8.2	10.9	1.33
7	35/65/1	46	90	100	22	8.6	7.5	10.3	1.13
8	50/50/1	38	99	100	28	8.5	8.0	10.1	1.19
9	65/35/1	31	61	100	49	5.8	3.9	4.6	1.13
10	80/20/1	25	70	100	59	5.9	2.5	2.7	1.44
11	90/10/1	13	79	100	60	5.5	1.3	1.4	1.59
12	100/0/1	8		100	100				

[a]Conditions: CTPB (0.02 mmol, 24 mg), −50 °C, 8 h, CTPB/U4/BDM = 1/1/1, THF was used as solvent, $[M]_0 = [EVP]_0 + [CL]_0 = 1.6$ M. [b]Determined by ^{1}H NMR spectroscopy. [c]EVP polymerization selectivity via ROP pathway determined by ^{1}H NMR spectroscopy. [d]$M_{n,theo.} = [EVP]_0/[I] \times conv.(EVP) \times M_{EVP} + [CL]_0/[I] \times conv.(CL) \times M_{CL} + M_{BDM}$. [e]$M_{n,NMR.}$ = Integration (6.95 to 6.80 ppm) × M_{EVP} + Integration/2 (4.15 to 4.00 ppm) × M_{CL} + M_{BDM}. [f]Determined by SEC in THF at 40 °C relative to PS standards. [g]Polymerization time: 24 h.

the obtained copolyesters. Both ^{1}H and ^{13}C NMR spectra indicate the successful synthesis of the desired linear poly(CL-*co*-EVP) copolyester. In a typical ^{1}H NMR spectrum of poly(CL-*co*-EVP) obtained in Table 1 run 6 (Figure 1A), signals at 6.84 (H_f), 5.79 (H_k), and 5.21 (H_l) ppm signify the protons of unsaturated C=C double bonds, consistent with the structure of linear poly(CL-*co*-EVP) copolyester. In addition, in the range of 6.95 to 6.80 ppm, two sets of quartet resonances are distinctly observed and centered at 6.90 and 6.84 ppm, respectively. In comparison to the ^{1}H NMR spectrum of poly(EVP)$_{ROP}$ homopolymer, the former signal is assigned to the ring-opening EVP-unit of EVP−EVP homosequence, while the latter one is attributed to that of EVP−CL heterosequence. Correspondingly, the other two sets of triplet signals (Figure 1A, H_e at 4.10 and 4.04 ppm) are also observed in the range of 4.15−4.00 ppm and attributed to the methylene group proximal to oxygen atom of CL within the CL−EVP heterosequence and CL−CL homosequence, respectively. As shown in Figure 1B, the methine carbon (C_m) proximal to the oxygen atom of EVP exhibits two signals at 74.23 and 74.19 ppm, relating to EVP−EVP homosequence and EVP−CL heterosequence, respectively. In addition, the methylene carbon (C_f) proximal to the oxygen atom of CL gives two peaks at 64.18 and 64.09 ppm, relating to EVP−CL heterosequence and CL−CL homosequence, respectively. These results clearly suggest a gradient poly(CL-*co*-EVP) structure.

The MALDI-TOF mass spectrum of the same sample is shown in Figure 1C and provides additional confirmation for the well-defined structure of the linear poly(CL-*co*-EVP) copolyester. The signals in the spectrum can be identified as a series of linear poly(CL-*co*-EVP) isomers with varying EVP and CL repeating units. The m/z values match well (with only a discrepancy of ∼1 in comparison to calculated values) the formula m/z = 138 (BDM) + 114.1x (CL) + 152.2y (EVP) + 23 (Na^+), where x and y represent the numbers of CL and EVP repeating units, respectively. Note that since 114.1 × 4 = 456.4 and 152.2 × 3 = 456.6, every peak can result from different compositions. Therefore, a specific structure cannot be uniquely determined by MALDI-TOF analysis. For example, the molar mass of 3355 could be assigned to multiple compositions, such as x/y = 20/6, 24/3, 16/9, or 12/12. However, all possibilities correspond to linear poly(CL-*co*-EVP) copolyesters with BDM as the initiator, fully consistent with the conclusions drawn from NMR analysis. The DOSY NMR spectrum (Figure 1D) shows only one single diffusion coefficient, further demonstrating that the resulting product is a true copolymer of EVP and CL rather than a mixture of poly(EVP) and PCL homopolymers.

2.2. Kinetic Study of Copolymerization of EVP and CL. To authenticate the monomer sequence of the resultant copolymers, kinetic studies were performed. During the copolymerization, a feed ratio of EVP/CL = 1/1 at −50 °C (Table S1), both EVP and CL conversions gradually increased over the polymerization time in the range of 0.2 to 4 h (Figure 2A), further confirming the gradient structure of poly(CL-*co*-EVP) copolyester. A notable linear correlation between the measured M_ns and the overall monomer conversions was evidenced (Figure 2B), while the distributions of the resulting poly(CL-*co*-EVP) copolyesters were monomodal and narrow ($Đ$ < 1.20), even at high monomer conversions (Figure 2C). These results suggest controlled ROCOP of EVP and CL by the binary CTPB/U4 catalytic system, which shows great potential to prepare well-defined poly(CL-*co*-EVP) copolyesters. Then, we endeavored to synthesize a series of poly(CL-*co*-EVP) copolyesters with varying M_ns by adjusting the monomer-to-initiator feeding ratios (Table 1, run 6 and Table 2, runs 1−3), while the incorporations of EVP in the products remained nearly unchanged. With an increase in the targeted degree of polymerization (DP) from 100 to 300, the measured M_ns of the resulting poly(CL-*co*-EVP) copolyesters by SEC demonstrated a linear increase from 10.8 to 22.6 kDa (Figure 2D). However, it was found that both $M_{n,SEC}$ and $M_{n,NMR}$ of the resultant polymer with high targeted DP were lower than the theoretical value, probably because the extended reaction time (24 h in Table 2, run 3) led to some unexpected side reactions. These side reactions were likely attributed to transesterification, as observing a slight widening of the SEC trace (Figure 2D, green trace) or initiation by the impurities from the large amounts of monomer and solvent used.

Reactivity ratios for the copolymerization of EVP with CL were calculated to gain deeper insights into the kinetic behavior. The copolymerization results of EVP with CL at various feeding molar ratios are collected in Table S2, and the reactivity ratios were determined using the Mayo−Lewis

https://doi.org/10.1021/acs.macromol.5c00076
Macromolecules 2025, 58, 3497−3508

Scheme 2. Synthesis of Bifunctional Copolyesters via Post-modifications of poly(CL-*co*-EVP) Copolymers

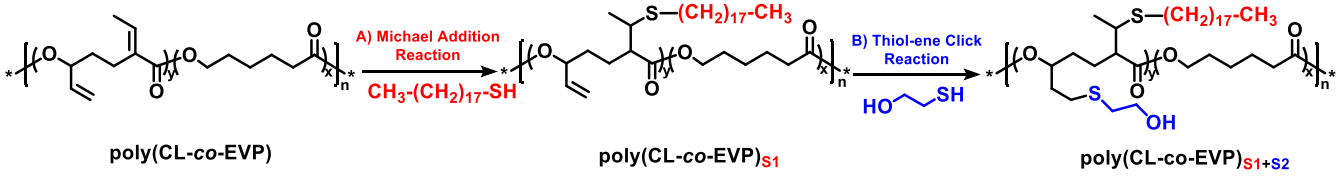

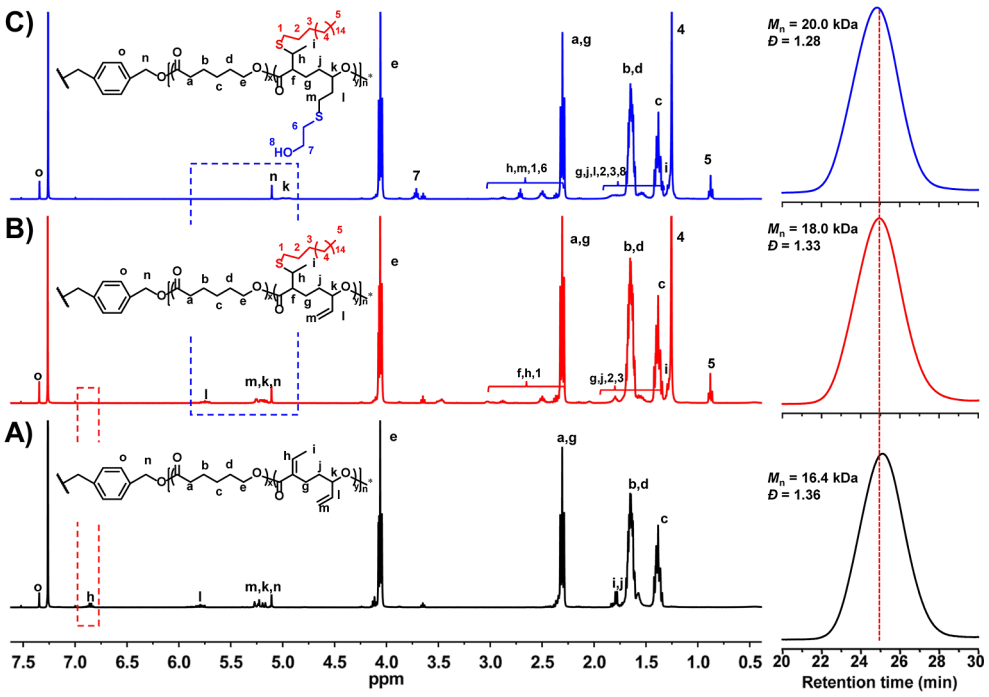

Figure 3. Stacked ^{1}H NMR spectra in $CDCl_3$ and SEC traces of (A) poly(CL-*co*-EVP) (M_n = 16.4 kDa, $Đ$ = 1.36, 8 mol % EVP), (B) poly(CL-*co*-EVP)$_{S1}$ produced via selective Michael addition reaction (M_n = 18.0 kDa, $Đ$ = 1.33), and (C) poly(CL-*co*-EVP)$_{S1+S2}$ produced via two sequential Michael addition and photoinduced thiol−ene click reactions (M_n = 20.0 kDa, $Đ$ = 1.28).

equation because only relatively high conversion of CL was obtained (>10%).[50] Figure S7 illustrates the intersection of five lines, yielding values of r_{EVP} = 0.17 and r_{CL} = 3.67. Previously, it was reported that the reactivity ratios of monomers in ROCOP of EtVP and CL were r_{EtVP} = 1.37 and r_{CL} = 0.91, indicating the formation of a somewhat random poly(CL-*co*-EtVP) copolymer with some gradient character. This difference in reactivity ratios can be attributed to the lower ceiling temperature (T_c = −141 °C at $[EVP]_0$ = 1 M) of EVP than that of EtVP (T_c = 18.3 °C at $[EtVP]_0$ = 1 M).[29,30] Considering that $r_{CL} \gg 1$ and $r_{EVP} \ll 1$, the resultant poly(CL-*co*-EVP) copolyesters are anticipated to have a gradient distribution of EVP and CL units with the majority of CL repeating units initially integrating into the polymer chain. For instance, the copolymerization of EVP with CL conducted at a feeding molar ratio of [EVP]/[CL] = 1/1 within 5 min yielded a gradient poly(CL-*co*-EVP) copolyester with 21 mol % EVP incorporation and 79 mol % CL incorporation, respectively (Table S2, run 3).

In addition, poly(CL-*co*-EVP) copolyesters with varying EVP incorporations and targeted DP of 100 were successfully prepared by using different feeding molar ratios of $[EVP]_0/[CL]_0$, and the results are shown in Table 2. As the ratios of $[EVP]_0/[CL]_0$ increased from 1/9 to 9/1, the EVP incorporations in the resulting poly(CL-*co*-EVP) copolyesters increased from 5 to 60 mol % (Table 2). However, copolyesters with high contents of EVP showed much lower M_ns by both NMR and SEC than that by theoretical calculation (Table 2, runs 10 and 11), probably because the high concentration of EVP led to chain transfer reactions, as evidenced by the broadened distributions ($Đ$ = 1.44 and 1.59). The EVP and CL sequence distribution are shown in Table S3 based on the peak integrations in the 165 to 175 ppm region of the quantitative ^{13}C NMR (Figures S8−S12). Thus, the chain structures of the poly(CL-*co*-EVP) copolyesters can be readily adjusted by altering the monomer feeding ratios.

2.3. Post-Modification of Poly(CL-*co*-EVP) Copolyesters. The obtained poly(CL-*co*-EVP) copolyesters contain two pendant C═C double bonds with distinct reactivity that can be functionalized through either a base-catalyzed thiol-Michael addition reaction or a phototriggered thiol−ene click reaction.[51,52] For example, postmodification of poly(CL-*co*-EVP) copolyester was achieved using 1-octadecanethiol via the thiol-Michael addition reaction (Scheme 2A), using DBU as the catalyst at room temperature. The obtained poly(CL-*co*-EVP)$_{s1}$ sample was carefully analyzed by ^{1}H NMR spectroscopy (Figures 3B and S13) and compared to that of poly(CL-*co*-EVP) copolyester (Figure 3A). The resonances from 6.95 to 6.80 ppm of protons on the internal double bond (H_h in Figure 3A) completely disappear, while two new resonances at 2.50 and 0.84 ppm (Figure 3B) are observed for the $-S-CH_2-(CH_2)_{16}-CH_3$ (H_1) and $-S-(CH_2)_{17}-CH_3$ (H_5) protons,

https://doi.org/10.1021/acs.macromol.5c00076
Macromolecules 2025, 58, 3497−3508

Table 3. Summary of Mechanical Properties of the Copolyesters

Sample	$M_{n,SEC}$ (kDa)[a]	$Đ$[a]	incorp.[b] (mol %)	σ_b (MPa)[c]	ε_b (%)[c]	E_y (MPa)[d]
PCL	38.9	1.60	0	17.4 ± 2.1	286 ± 49	2.3 ± 0.5
poly(CL-*co*-EVP)-2%	44.7	1.86	2	28.5 ± 1.8	883 ± 65	2.2 ± 0.5
poly(CL-*co*-EVP)-2%-cross-link				13.0 ± 1.4	276 ± 65	1.1 ± 0.2
poly(CL-*co*-EVP)-10%	41.4	1.66	10	16.4 ± 2.0	629 ± 44	1.1 ± 0.5
poly(CL-*co*-EVP)-10%-cross-link				1.5 ± 0.7	29 ± 11	0.09 ± 0.02

[a]Determined by SEC in THF at 40 °C relative to PS standards. [b]Incorporation of EVP determined by ^{1}H NMR spectroscopy. [c]ε_b, elongation at break; σ_b, tensile strength. [d]Young's modulus E_y were calculated as the slope of stress−strain curves at strain below 5%.

respectively. These results reveal the successful preparation of monofunctionalized copolyester with octadecyl mercaptan through selective Michael addition.

Subsequently, the terminal alkene underwent a photoinduced thiol−ene click reaction with 2-mercaptoethanol (Scheme 2B) in the presence of DMPA. This process led to the incorporation of the second functional group and, thus, afforded a novel bifunctional copolyester (Figure 3B). It is evidenced by the disappearance of the original signal at 5.67 (H_l) ppm for the terminal alkene (Figures 3C and S14). The mono- and bifunctional poly(CL-*co*-EVP) copolyesters were further characterized by SEC analysis (Figure 3, right), revealing a step-by-step increase in M_ns (Figure S15). This stepwise strategy enables the synthesis of a variety of bifunctional PCL, providing them with a diverse range of properties that are unattainable through previous PCL functionalization efforts.[53−55] For comparison, the recently reported poly(EtVP-*co*-CL) containing one type of unsaturated double bond cannot achieve such a precise bifunctional structure through postmodification.[27]

Next, cross-linked polyesters (poly(CL-*co*-EVP)-2%-cross-link and poly(CL-*co*-EVP)-10%-cross-link) were synthesized from poly(CL-*co*-EVP) precursors with 2 and 10 mol % EVP incorporations, using trimethylolpropane tris(3-mercaptopropionate) (TMPT) as the cross-linking agent. The mechanical properties of poly(CL-*co*-EVP) copolyesters, both with and without cross-linking, were subsequently evaluated using uniaxial tensile tests at a strain rate of 5 mm min^{-1}. Films were prepared through a solvent-casting technique and then cut into dumbbell-shaped specimens for testing (Figure S16). The tensile strength (σ_b), elongation at break (ε_b), and Young's moduli (E_y) were determined from tests on at least three specimens (Figures S17−S21) and are presented in Table 3 as average values with standard deviations. In addition, the mechanical properties of PCL homopolymer with a similar M_n (M_n = 38.9 kDa) were also examined for comparison, showing a tensile strength (σ_b) of 17.4 ± 2.1 MPa and an elongation at break (ε_b) of 286 ± 49%. This relatively low ε_b of ∼300% compared to the literature values of 600 to 1600% is presumably a combined effect of the low molar mass and high crystallinity of the PCL reference used in our study. According to the previous studies on the molar mass-tensile relationship of PCL,[56,57] it is probable that the brittle-to-ductile transition molar mass of PCL lies close to 40 kDa under room temperature. Though at least 10 times of their critical entanglement molar mass ($M_{ce,PCL}$ = 2−4 kg/mol),[58−62] the PCL chains of 38.9 kDa do not contain sufficient amount of long tie molecules that allow for effective entanglement in the amorphous region of PCL, and therefore they have ramifications on the stress propagation within the resulting materials. Remarkably, only 2 mol % incorporation of EVP resulted in a significant improvement in both σ_b and ε_b to 28.5 ± 1.8 MPa and 883 ± 65%, respectively. It is somewhat surprising that one EVP insertion per 50 PCL monomers can dramatically enhance the extensibility of the materials, especially considering that the crystallinity remains almost the same between the two (Figure S22a,b, and Table S4);[63] however, this toughening effect can be rationalized by the decrease in the spherulite size[64] in poly(CL-*co*-EVP)-2% compared with the neat PCL, which to some extent prevents the stress from concentrating on the impinging spherulite boundaries (see the polarized optical microscopy images in Figures S23 and S24). Further increasing the EVP content to 10 mol % led to reduction in both strength and elongation (σ_b = 16.4 ± 2.0 MPa, ε_b = 629 ± 44%), concomitant with the decrease in PCL crystallinity (Figure S22d and Table S4). Overall, compared with PCL homopolymer, its copolymer counterparts, poly(CL-*co*-EVP)-2% and poly(CL-*co*-EVP)-10% contain 2 mol % (Figure S25) and 10 mol % EVP (Figure S26) monomers that are (mostly) randomly distributed along the polymer chains. Such random insertions compromise the crystallinity of the resulting thermoplastic materials, and the materials gradually undergo a "plastic-to-viscoelastic" transition, as characterized by a decrease in Young's moduli and the diminishing of the yielding behaviors (Figure 4, green curve).

Subsequently, the effects of cross-linking were investigated. For the sample of poly(CL-*co*-EVP)-2%-cross-link with 2 mol

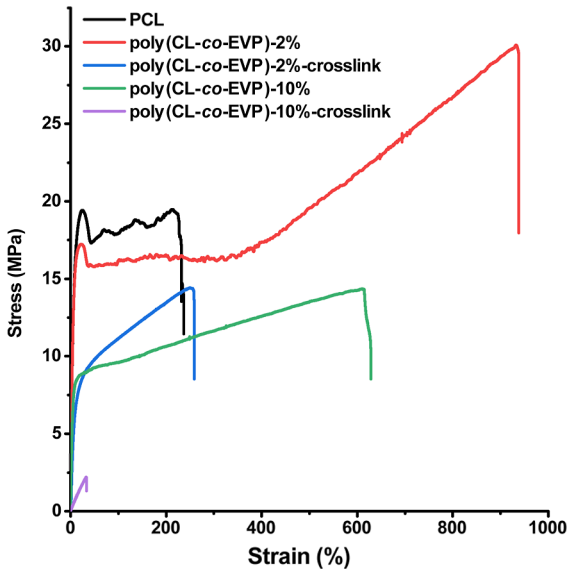

Figure 4. Stress−strain curves of PCL homopolymer (black line, M_n = 38.9 kDa, $Đ$ = 1.60), poly(CL-*co*-EVP)-2% (red line, M_n = 44.7 kDa, $Đ$ = 1.86, 2 mol % EVP incorporation), poly(CL-*co*-EVP)-2%-cross-link (blue line), poly(CL-*co*-EVP)-10% (green line, M_n = 41.4 kDa, $Đ$ = 1.66, 10 mol % EVP incorporation) and poly(CL-*co*-EVP)-10%-cross-link (purple line).

https://doi.org/10.1021/acs.macromol.5c00076
Macromolecules 2025, 58, 3497−3508

% EVP incorporation, as shown in Figure 4 (blue), the material has moderate tensile strength (σ_b = 13.0 ± 1.4 MPa) and elongation at break (ε_b = 276 ± 65%) and exhibits properties akin to elastomers, showing no yielding behaviors at all. In contrast, for the poly(CL-*co*-EVP)-10%-cross-link sample with 10 mol % EVP incorporation (Figure 4, purple), cross-linking significantly reduces both strength and elongation at break (σ_b = 1.5 ± 0.7 MPa, ε_b = 29 ± 11%). Thus, poly(CL-*co*-EVP)-2%-cross-link (with 2 mol % EVP fully cross-linked) has superior tensile strength and elongation at break than poly(CL-*co*-EVP)-10%-cross-link (with 10 mol % EVP fully cross-linked). In the latter circumstance, the polymer is already densely cross-linked (1 cross-link per 10 monomers); at this point, the mobility of polymer chains becomes highly restricted, and the excessively cross-linked network is unable to dissipate deformation energy effectively through molecular motion, therefore resulting in brittleness and ease of cracking at low elongation, reminiscent of thermosets. By contrasting the cross-linked and pristine poly(CL-*co*-EVP) samples, we can conclude that the incorporation of 2 mol % EVP markedly enhances the plasticity and extensibility of the neat PCL, while cross-linking of the EVP motives transforms these plastic materials to elastomeric ones.

2.4. Thermodynamic Properties of Copolyesters. The thermal stability of poly(CL-*co*-EVP) samples on a broader composition window was analyzed by thermal gravimetric analysis (TGA) and differential scanning calorimetry (DSC). Supporting Information Figure S27 compares TGA curves and relative derivative thermogravimetry (DTG) curves of the copolymer poly(CL-*co*-EVP) as well as the homopolymers PCL and poly(EVP). The poly(CL-*co*-EVP) copolyester displays one-step degradation steps and good thermal stability with a 5% weight loss at 340.5 °C and $T_{d,\,95\%}$ at 459.0 °C (Figure S27, red curves). The overlay plots show that poly(CL-*co*-EVP) copolyester exhibits thermal stability rather similar to that of the homopolymer PCL and is more stable than the homopolymer poly(EVP). On the other hand, the mono-functionalized poly(CL-*co*-EVP)$_{S1}$ displays a one-step decomposition profile with a $T_{d,\,5\%}$ at 304.4 °C and $T_{d,\,95\%}$ at 440.5 °C (Figure S28, red), while the bifunctionalized poly(CL-*co*-EVP)$_{S1+S2}$ shows a $T_{d,\,5\%}$ at 348.7 °C and $T_{d,\,95\%}$ at 440.5 °C (Figure S28, blue).

Figure 5 displays the stacked second heating scans of DSC curves of poly(CL-*co*-EVP) copolyesters with EVP incorporations varied from 5 to 60 mol %, plotted in juxtaposition with those of PCL and poly(EVP) homopolymers. At the two ends, PCL homopolymer gives a single melting transition (T_m) at 55.1 °C (Figure 5, bottom), while poly(EVP) homopolymer is amorphous indicated by the absence of crystallization and melting transition peaks in the DSC curve (Figure 5, top). In between the two cases, the poly(CL-*co*-EVP) copolyesters display composition-dependent thermal behaviors (Figure 5 and S29; Table S5), and it is interesting that over the EVP molar composition of 5−22%, all poly(CL-*co*-EVP) copolyesters display major melting peaks at 28−46 °C and minor melting peaks that are about 10 °C below the former. The presence of two melting peaks is probably caused by the small, incomplete crystals originating from the depressed crystallization rate of poly(CL-*co*-EVP) upon cooling, and thus their fast recrystallization upon melting.[16,65] These results indicate that the crystallinities of poly(CL-*co*-EVP) copolyesters gradually decrease with the incorporation of EVP and finally completely vanish at EVP molar compositions over 49%.

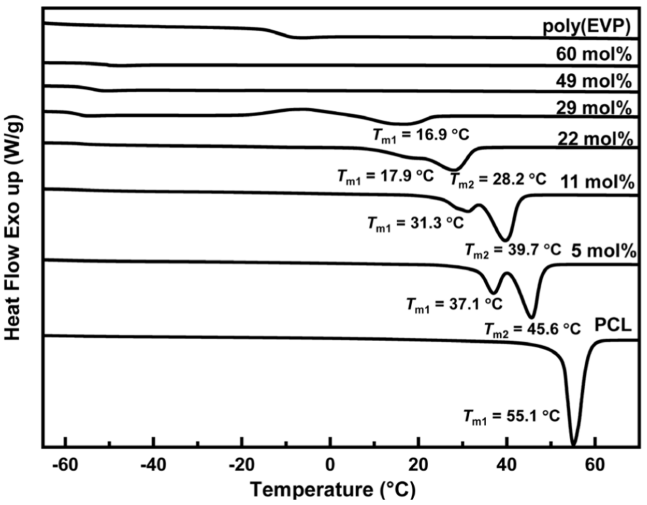

Figure 5. Second heating scans of DSC curves of poly(CL-*co*-EVP) copolyesters with varied EVP incorporations (copolyester samples obtained in Table 2; PCL, M_n = 21.6 kDa, $Đ$ = 1.59; poly(EVP), M_n = 6.5 kDa, $Đ$ = 1.19).

3. CONCLUSIONS

The chemoselective ROCOPs of EVP with CL have been achieved with a CTPB/urea binary catalyst, which exclusively yield the linear and gradient poly(CL-*co*-EVP) copolyesters with narrow distributions ($Đ$ < 1.2 for most cases), and wide range of EVP-contents (0−60 mol %). It was remarkable that chemoselective ROP of EVP in the copolymerization was even achieved at room temperature, thanks to the introduction of the second monomer (CL) increased the entropy (ΔS) and decreased the Gibbs free energy (ΔG) of the polymerization system. The catalytic activity and chemoselectivity were highly affected by the nature of the ureas and the polymerization conditions. Remarkably, an EVP conversion up to 55% was achieved for ROCOP of EVP with CL, much higher than that for homopolymerization of EVP. The well-defined structure of the resulting copolyester was confirmed by comprehensive characterizations using 1D and 2D NMR, MALDI-TOF MS, DOSY NMR, and SEC techniques. Kinetic studies supported a gradient propagation of EVP and CL, and the reactivity ratios of EVP and CL were determined as 0.17 and 3.67, respectively. Notably, the obtained poly(CL-*co*-EVP) copolyesters contained two pendent C = C double bonds with distinct reactivity and thus can be easily and selectively postfunctionalized to produce bifunctional polyesters. Mechanical properties indicated that the incorporation of only 2 mol % EVP significantly enhanced the mechanical characteristics of homopolymer PCL, while cross-linking facilitated the transformation of PCL from thermoplastics to elastomers. The thermal behaviors of the poly(CL-*co*-EVP) copolyesters strongly depended on their compositions and functionalizations. This study offers a simple strategy to synthesize well-defined bifunctional copolyesters from CO_2 with 1,3-butadiene and may inspire further exploration of their applications.

4. EXPERIMENTAL SECTION

4.1. Materials. The monomer EVP was prepared according to the previously reported procedure,[1] dried over CaH_2 for 24 h, and distilled under reduced pressure. CL was purchased from Aladdin Co. and stirred with CaH_2 for 24 h. THF was purified by first purging with dry nitrogen, then by passing through columns of activated alumina. 1-Octadecanethiol (97%) was obtained from Macklin, and 2-

https://doi.org/10.1021/acs.macromol.5c00076
Macromolecules 2025, 58, 3497−3508

mercaptoethanol (98%) was obtained from Aladdin Co., 2,2-dimethoxy-2-phenylacetophenone (DMPA, 98%) from Energy Chemical Co. Benzenedimethanol (BDM) was purchased from TCI and recrystallized from toluene period to used. CTPB and ureas (U1−U4) were synthesized according to the literature.[66,67] All other chemicals were purchased from commercial suppliers and used without further purification, unless otherwise noted.

4.2. Instruments. NMR spectra were recorded on a Bruker AVANCE NEO 400 MHz NMR spectrometer (400 MHz for ^{1}H NMR, 100 MHz for ^{13}C NMR). ^{1}H detected HMBC and HSQC techniques were used to assist in the assignment of the ^{1}H and ^{13}C NMR spectra. The molar mass (M_n) and dispersity ($Đ = M_w/M_n$) were determined by SEC equipped with an Agilent HPLC system, a 1260 Hip degasser, a 1260 Iso pump, and a 1260 differential refractometer detector. One PLgel 5 μm guard column and three Mz-Gel SD$_{plus}$ (10^3 Å, 10^4 Å, and 10^5 Å) columns were connected in series. The SEC columns were eluted with THF at 1.0 mL/min at 40 °C. The sample concentration used for SEC analysis was 5 mg/mL. Matrix-assisted laser desorption/ionization time-of-flight mass spectroscopy (MALDI-TOF MS) analyses were conducted on a Bruker Microflex MALDI-TOF MS spectrometer equipped with a 337 nm nitrogen laser. *Trans*-2-[3-(4-*tert*-butylphenyl)-2-methyl-2-propenylidene]-malononitrile (DCTB) was used as the matrix, and CF_3COONa was used as the ionization agent. DSC was performed using a TA DSC 25 differential scanning calorimeter that was calibrated using high purity indium. Measurements were performed under N_2 atmosphere with a flow rate of 50 mL/min. Each sample with a mass of 5−10 mg was used for the measurement. T_gs were determined from the second scan at a heating rate of 5 °C/min following a slow cooling rate of 5 °C/min to remove the influence of the thermal history. Thermogravimetric analysis (TGA) measurements were performed on a STA 800 thermogravimetric analyzer. The samples were heated from room temperature to 600 °C at a heating rate of 10 °C/min under a N_2 atmosphere with a flow rate of 40 mL/min. The postfunctionalization experiments were carried out in an ultraviolet lamp box, using an ultraviolet high-pressure mercury lamp (GGZ250) with a wavelength of 365 nm and a power of 250 W. The tensile stress−strain curves of all stretch splines were obtained at room temperature using a universal testing machine (Instron3360) with a tensile rate of 5 mm/min. The stretched spline had a neck length of 20 mm, a width of 4 mm, and a thickness of 0.3 mm. All tests were conducted in triplicate, and the median values were reported to minimize the influence of incidental factors. The morphologies were observed using an Axioskop 40A optical microscope (Beijing Younake Technology Co., Ltd.). All of the presented pictures were taken under crossed polarizers.

4.3. General Procedure for the Copolymerization of EVP and CL (Table 1, run 6). In a glovebox, CTPB (0.02 mmol, 24 mg), BDM (0.02 mmol, 2.8 mg), and U4 (0.02 mmol, 12.0 mg) were mixed in 1 mL of THF in a Schlenk tube. After equilibrium at −50 °C, the mixtures of CL (1.0 mmol, 0.11 mL) and EVP (1.0 mmol, 0.13 mL) were added into the Schlenk tube to begin the polymerization. After the desired reaction time, a few drops of acetic acid in chloroform were added to quench the reaction, and a small portion of the solution was taken and used to determine the polymerization selectivity and the conversion of EVP and CL by ^{1}H NMR. The conversion of the EVP monomer was calculated based on the integration (I) ratio $I_{poly(EVP)}/[I_{poly(EVP)} + I_{EVP}]$ of the protons of unsaturated C=C double bonds of poly(EVP) (6.94−6.77 ppm) and EVP (7.17−7.07 ppm), while the conversion of CL was calculated by the ratio of $I_{PCL}/[I_{PCL} + I_{CL}]$ of the methylene protons ($-OCH_2$) of PCL (4.15−3.97 ppm) and CL (4.23 ppm). The selectivity of the EVP monomer was calculated based on the integration (I) ratio $I_{poly(EVP)}/[I_{poly(EVP)} + I_{Di\text{-}EVP}]$ of the protons of unsaturated C=C double bonds of poly(EVP) (6.94−6.77 ppm) and Di-EVP (7.04−6.95 ppm). The remaining solution was poured into cold methanol to precipitate the polymer, which was dried overnight under a vacuum in an oven. The resulting polymer was analyzed by SEC, DSC, and TGA. ^{1}H NMR (400 MHz, $CDCl_3$): δ 7.34 (s, 4H, Ar−H of initiator), 6.94−6.77 (m, 13H), 5.89−5.75 (m, 13H), 5.34−5.08 (m, 42H), 4.15−3.97 (m, 100H), 2.40−2.23 (m, 120H), 1.84−1.74 (m, 45H), 1.70−1.48 (m, 234H), 1.47−1.30 (m, 103H) ppm. ^{13}C NMR (100 MHz, $CDCl_3$): δ 173.51, 167.49, 141.00, 138.16, 137.79, 136.31, 132.36, 128.29, 116.80, 114.47, 74.22, 71.90, 65.83, 64.21, 36.29, 34.09, 33.26, 28.32, 25.50, 24.65, 22.14, 14.16 ppm. M_n = 10.8 kDa, $Đ$ = 1.19, T_g = −57.0 °C, T_m = 16.9 °C, T_c = −6.0 °C, $T_{d,\,5\%}$ = 275.2 °C, and $T_{d,\,95\%}$ = 494.2 °C.

4.4. Preparation of Poly(CL-*co*-EVP)$_{S1}$ via Michael Addition Reaction. A mixture of 400 mg of poly(CL-*co*-EVP) (M_n = 16.4 kDa, 8 mol % EVP), 720 mg of 1-octadecanethiol (2.5 mmol, 7 equiv), and 25 μL of DBU (0.17 mmol, 0.6 equiv) was dissolved in 1.2 mL of chloroform. The reaction mixture was stirred at 20 °C for 24 h. An aliquot of the solution was withdrawn and used to determine the conversion by ^{1}H NMR. The remaining mixture was poured into excess hexane. Poly(CL-*co*-EVP)$_{S1}$ was obtained as a precipitate, which was washed twice with hexane and then dried under a vacuum at room temperature. The resulting polymer was analyzed by SEC, DSC, and TGA. M_n = 18.0 kDa, $Đ$ = 1.33, T_g = −55.8 °C, T_{m1} = 4.8 °C, T_{m2} = 46.0 °C, T_c = −13.1 °C, $T_{d,\,5\%}$ = 304.4 °C, and $T_{d,\,95\%}$ = 440.5 °C.

4.5. Preparation of Poly(CL-*co*-EVP)$_{S1+S2}$ via Thiol−Ene Click Reaction. A flame-dried Schlenk tube was charged with 170 mg of poly(CL-*co*-EVP)$_{S1}$, 6.8 mg (0.026 mmol, 4 wt %) DMPA, and 0.5 mL of chloroform, and then, 21 μL of 2-mercaptoethanol (0.29 mmol, 3 equiv) was added into the Schlenk tube via a gastight syringe. The tube was then irradiated by UV light at 365 nm for 4 h. The reaction mixture was poured into excess cold methanol, and the precipitate obtained was washed twice with excess cold methanol and then dried under vacuum at room temperature. The resulting polymer was analyzed by SEC, DSC, and TGA. M_n = 20.0 kDa, $Đ$ = 1.28, T_g = −55.3 °C, T_{m1} = 4.4 °C, T_{m2} = 45.0 °C, T_c = −14.7 °C, $T_{d,\,5\%}$ = 348.7 °C, and $T_{d,\,95\%}$ = 440.5 °C.

4.6. Preparation of Poly(CL-*co*-EVP)-2%. In a glovebox, CTPB (0.02 mmol, 24 mg), BDM (0.08 mmol, 11.2 mg), and U4 (0.02 mmol, 12 mg) were mixed in 2 mL of THF in a Schlenk tube. After equilibrium at 0 °C, the mixtures of CL (3.6 mmol, 0.40 mL) and EVP (0.4 mmol, 0.05 mL) was added into the Schlenk tube to begin the polymerization. After 6 h, a few drops of acetic acid in chloroform were added to quench the reaction, and a small portion of the solution was taken and used to determine the polymerization selectivity and the conversion of EVP and CL by ^{1}H NMR. The remaining solution was poured into cold methanol to precipitate the polymer, which was dried overnight under vacuum in an oven. The resulting polymer was analyzed by ^{1}H NMR, SEC, and DSC. EVP incorporation = 2 mol %; M_n = 44.7 kDa, $Đ$ = 1.86; T_m = 53.7 °C.

4.7. Preparation of Poly(CL-*co*-EVP)-10%. In a glovebox, CTPB (0.04 mmol, 48 mg), BDM (0.08 mmol, 11.2 mg), and U4 (0.04 mmol, 24 mg) were mixed in 2.5 mL of THF in a Schlenk tube. After equilibrium at 0 °C, the mixtures of CL (2.6 mmol, 0.29 mL) and EVP (1.4 mmol, 0.18 mL) were added into the Schlenk tube to begin the polymerization. After 8 h, a few drops of acetic acid in chloroform were added to quench the reaction and a small portion of the solution was taken and used to determine the polymerization selectivity and the conversion of EVP and CL by ^{1}H NMR. The remaining solution was poured into cold methanol to precipitate the polymer, which was dried overnight under vacuum in an oven. The resulting polymer was analyzed by ^{1}H NMR, SEC, and DSC. EVP incorporation = 10 mol %; M_n = 41.4 kDa, $Đ$ = 1.66; T_{m1} = 36.8 °C, T_{m2} = 41.9 °C.

4.8. General Procedure for the Cross-Linked Polyesters. 500 mg of poly(CL-*co*-EVP) (M_n = 44.7 kDa, 2 mol % of EVP incorporation), 8 μL of trimethylolpropane tris(3-mercaptopropionate) (TMPT), and 20 mg of DMPA were dissolved in 3 mL of $CHCl_3$. The solution was poured into a polytetrafluoroethylene (PTFE) mold and allowed to evaporate for 4 h to obtain a viscous liquid. The viscous liquid was then irradiated under UV light (365 nm) at room temperature for 0.5 h. The poly(CL-*co*-EVP)-2%-cross-link sample was finally obtained after further drying at room temperature under high vacuum.

https://doi.org/10.1021/acs.macromol.5c00076
Macromolecules 2025, 58, 3497−3508

■ ASSOCIATED CONTENT

Supporting Information

The Supporting Information is available free of charge at https://pubs.acs.org/doi/10.1021/acs.macromol.5c00076.

NMR spectra, SEC, MALDI TOF and DSC analyses of polymer materials, computational details (PDF)

■ AUTHOR INFORMATION

Corresponding Authors

Shaofeng Liu − *Key Laboratory of Biobased Polymer Materials, College of Polymer Science and Engineering, Qingdao University of Science and Technology, Qingdao 266042, China;* orcid.org/0000-0002-1230-0946; Email: shaofengliu@qust.edu.cn

Zhibo Li − *Key Laboratory of Biobased Polymer Materials, College of Polymer Science and Engineering, Qingdao University of Science and Technology, Qingdao 266042, China; Key Laboratory of Optic-electric Sensing and Analytical Chemistry for Life Science, MOE, College of Chemistry and Molecular Engineering, Qingdao University of Science and Technology, Qingdao 266042, China;* orcid.org/0000-0001-9512-1507; Email: zbli@qust.edu.cn

Authors

Junhao Shen − *Key Laboratory of Biobased Polymer Materials, College of Polymer Science and Engineering, Qingdao University of Science and Technology, Qingdao 266042, China*

Jinbo Zhang − *Key Laboratory of Biobased Polymer Materials, College of Polymer Science and Engineering, Qingdao University of Science and Technology, Qingdao 266042, China*

Wenhui Kong − *Key Laboratory of Biobased Polymer Materials, College of Polymer Science and Engineering, Qingdao University of Science and Technology, Qingdao 266042, China*

Yuanchi Ma − *Key Laboratory of Biobased Polymer Materials, College of Polymer Science and Engineering, Qingdao University of Science and Technology, Qingdao 266042, China*

Complete contact information is available at: https://pubs.acs.org/10.1021/acs.macromol.5c00076

Author Contributions

§J. S. and J. Z. contributed equally to this work. Shaofeng Liu, and Zhibo Li conceived the idea and designed the experiments. Junhao Shen, Jinbo Zhang, Wenhui Kong, and Yuanchi Ma performed the experiments and analyzed and processed the data. The manuscript was written through contributions of all authors. All authors have given approval to the final version of the manuscript.

Notes

The authors declare no competing financial interest.

■ ACKNOWLEDGMENTS

This work was supported by the National Key R&D Program of China (2021YFA1501600), Ministry of Education of the People's Republic of China, the National Natural Science Foundation of China (22031005, 22405154), and the Shandong Province Natural Science Foundation (no. ZR2024JQ015).

■ REFERENCES

(1) Yang, Z.; Shen, C.; Dong, K. Hydroxyl Group-Enabled Highly Efficient Ligand for Pd-Catalyzed Telomerization of 1,3-Butadiene with CO_2. *Chin. J. Chem.* **2022**, *40*, 2734−2740.

(2) Zhao, Z.; Shen, Y.; Kou, X.; Shi, J.; Wang, R.; Liu, F.; Li, Z. Organocatalytic Ring-Opening Copolymerization of Biorenewable α-Methylene-γ-butyrolactone toward Functional Copolyesters: Preparation and Composition Dependent Thermal Properties. *Macromolecules* **2020**, *53*, 3380−3389.

(3) Sharif, M.; Jackstell, R.; Dastgir, S.; Al-Shihi, B.; Beller, M. Efficient and selective Palladium-catalyzed Telomerization of 1,3-Butadiene with Carbon Dioxide. *ChemCatChem* **2017**, *9*, 542−546.

(4) Song, J.; Feng, X.; Yamamoto, Y.; Almansour, A. I.; Arumugam, N.; Kumar, R. S.; Bao, M. Selective Synthesis of δ-Lactone via Palladium Nanoparticles-Catalyzed Telomerization of CO_2 with 1,3-Butadiene. *Tetrahedron Lett.* **2016**, *57*, 3163−3166.

(5) Braunstein, P.; Matt, D.; Nobel, D. Carbon Dioxide Activation and Catalytic Lactone Synthesis by Telomerization of Butadiene and Carbon Dioxide. *J. Am. Chem. Soc.* **1988**, *110*, 3207−3212.

(6) Behr, A.; Juszak, K.-D. Palladium-catalyzed Reaction of Butadiene and Carbon Dioxide. *J. Organomet. Chem.* **1983**, *255*, 263−268.

(7) Musco, A.; Perego, C.; Tartiari, V. Telomerization Reactions of Butadiene and CO_2 Catalyzed by Phosphine Pd(0) Complexes: (E)-2-Ethylidenehept-6-en-5-olide and Octadienyl Esters of 2-Ethylidenehepta-4,6-dienoic Acid. *Inorg. Chim. Acta* **1978**, *28*, 147−148.

(8) Inoue, Y.; Sasaki, Y.; Hashimoto, H. Incorporation of CO_2 in Butadiene Dimerization Catalyzed by Palladium Complexes. Formation of 2-Ethylidene-5-hepten-4-olide. *Bull. Chem. Soc. Jpn.* **1978**, *51*, 2375−2378.

(9) Tang, S.; Lin, B.-L.; Tonks, I.; Eagan, J. M.; Ni, X.; Nozaki, K. Sustainable Copolymer Synthesis from Carbon Dioxide and Butadiene. *Chem. Rev.* **2024**, *124*, 3590−3607.

(10) Chen, K.; Mei, Y.; Zhang, Z.; Ling, J.; Ni, X. How to Open the Ring of a Di-ene-Substituted-δ-Valerolactone: From Carbon Dioxide and 1,3-Butadiene to Functional Polyesters. *ChemPlusChem* **2023**, *88*, No. e202300022.

(11) Tang, S.; Nozaki, K. Advances in the Synthesis of Copolymers from Carbon Dioxide, Dienes, and Olefins. *Acc. Chem. Res.* **2022**, *55*, 1524−1532.

(12) Rapagnani, R. M.; Tonks, I. A. 3-Ethyl-6-vinyltetrahydro-2H-pyran-2-one (EVP): a Versatile CO_2-Derived Lactone Platform for Polymer Synthesis. *Chem. Commun.* **2022**, *58*, 9586−9593.

(13) Eagan, J. M. The Divergent Reactivity of Lactones Derived from Butadiene and Carbon Dioxide in Macromolecular Synthesis. *Macromol. Rapid Commun.* **2022**, *44*, 2200348.

(14) Nozaki, K. New Polymers Made from Carbon Dioxide and Alkenes. *Bull. Chem. Soc. Jpn.* **2021**, *94*, 984−988.

(15) Liu, Y.; Lu, X.-B. Current Challenges and Perspectives in CO_2-Based Polymers. *Macromolecules* **2023**, *56*, 1759−1777.

(16) Kuang, Q.; Zhang, R.; Zhou, Z.; Liao, C.; Liu, S.; Chen, X.; Wang, X. A Supported Catalyst that Enables the Synthesis of Colorless CO_2-Polyols with Ultra-Low Molecular Weight. *Angew. Chem., Int. Ed.* **2023**, *62*, No. e202305186.

(17) Grignard, B.; Gennen, S.; Jérôme, C.; Kleij, A. W.; Detrembleur, C. Advances in the use of CO_2 as a Renewable Feedstock for the Synthesis of Polymers. *Chem. Soc. Rev.* **2019**, *48*, 4466−4514.

(18) Zhu, Y.; Romain, C.; Williams, C. K. Sustainable Polymers from Renewable Resources. *Nature* **2016**, *540*, 354−362.

(19) Aresta, M.; Dibenedetto, A.; Angelini, A. Catalysis for the Valorization of Exhaust Carbon: from CO_2 to Chemicals, Materials, and Fuels. Technological Use of CO_2. *Chem. Rev.* **2014**, *114*, 1709−1742.

(20) Haack, V.; Dinjus, E.; Pitter, S. Synthesis of Polymers with an Intact Lactone Ring Structure in the Main Chain. *Angew. Makromol. Chem.* **1998**, *257*, 19−22.

(21) Nakano, R.; Ito, S.; Nozaki, K. Copolymerization of Carbon Dioxide and Butadiene via a Lactone Intermediate. *Nat. Chem.* **2014**, *6*, 325−331.
(22) Hill, M. R.; Tang, S.; Masada, K.; Hirooka, Y.; Nozaki, K. Incorporation of CO_2-Derived Bicyclic Lactone into Conventional Vinyl Polymers. *Macromolecules* **2022**, *55*, 3311−3316.
(23) Tang, S.; Zhao, Y.; Nozaki, K. Accessing Divergent Main-Chain-Functionalized Polyethylenes via Copolymerization of Ethylene with a CO_2/Butadiene-Derived Lactone. *J. Am. Chem. Soc.* **2021**, *143*, 17953−17957.
(24) Liu, M.; Sun, Y.; Liang, Y.; Lin, B.-L. Highly Efficient Synthesis of Functionalizable Polymers from a CO_2/1,3-Butadiene-Derived Lactone. *ACS Macro Lett.* **2017**, *6*, 1373−1378.
(25) Garcia Espinosa, L. D.; Williams-Pavlantos, K.; Turney, K. M.; Wesdemiotis, C.; Eagan, J. M. Degradable Polymer Structures from Carbon Dioxide and Butadiene. *ACS Macro Lett.* **2021**, *10*, 1254−1259.
(26) Rapagnani, R. M.; Dunscomb, R. J.; Fresh, A. A.; Tonks, I. A. Tunable and recyclable polyesters from CO2 and butadiene. *Nat. Chem.* **2022**, *14*, 877−883.
(27) Anderson, R. J.; Fine, R. L.; Rapagnani, R. M.; Tonks, I. A. Ring-Opening Copolymerizations of a CO_2-Derived δ-Valerolactone with ε-Caprolactone and l-Lactide. *Macromolecules* **2024**, *57*, 6248−6254.
(28) Lou, Y.; Xu, L.; Gan, N.; Sun, Y.; Lin, B. L. Chemically Recyclable Polyesters from CO_2, H_2, and 1,3-Butadiene. *Innovation* **2022**, *3*, 100216.
(29) Lou, Y.; Xu, J.; Xu, L.; Chen, Z.; Lin, B.-L. Chemically Recyclable CO_2-Based Solid Polyesters with Facile Property Tunability. *Macromol. Rapid Commun.* **2022**, *43*, 2200341.
(30) Zhang, J.; Jiang, L.; Liu, S.; Shen, J.; Braunstein, P.; Shen, Y.; Kang, X.; Li, Z. Bifunctional and Recyclable Polyesters by Chemoselective Ring-Opening Polymerization of a δ-Lactone Derived from CO_2 and Butadiene. *Nat. Commun.* **2024**, *15*, 8698.
(31) Xu, J.; Niu, Y.; Lin, B.-L. Monomer-Recyclable Polyester from CO_2 and 1,3-Butadiene. *Macromol. Rapid Commun.* **2024**, *45*, 2400163.
(32) Hardouin Duparc, V.; Shakaroun, R. M.; Slawinski, M.; Carpentier, J.-F.; Guillaume, S. M. Ring-Opening (co)Polymerization of Six-Membered Substituted δ-Valerolactones with Alkali Metal Alkoxides. *Eur. Polym. J.* **2020**, *134*, 109858.
(33) Schneiderman, D. K.; Hillmyer, M. A. Aliphatic Polyester Block Polymer Design. *Macromolecules* **2016**, *49*, 2419−2428.
(34) Song, Q.; Pascouau, C.; Zhao, J.; Zhang, G.; Peruch, F.; Carlotti, S. Ring-Opening Polymerization of γ-Lactones and Copolymerization with Other Cyclic Monomers. *Prog. Polym. Sci.* **2020**, *110*, 101309.
(35) Wei, C.; Kou, X.; Liu, S.; Li, Z. Fast, Selective and Metal-Free Ring-Opening Polymerization to Synthesize Polycarbonate/Polyester Copolymers with High Incorporation of Ethylene Carbonate Using an Organocatalytic Phosphazene Base. *Polym. Chem.* **2019**, *10*, 5905−5912.
(36) Danko, M.; Basko, M.; Ďurkáčová, S.; Duda, A.; Mosnáček, J. Functional Polyesters with Pendant Double Bonds Prepared by Coordination−Insertion and Cationic Ring-Opening Copolymerizations of ε-Caprolactone with Renewable Tulipalin A. *Macromolecules* **2018**, *51*, 3582−3596.
(37) Hong, M.; Tang, X.; Newell, B. S.; Chen, E. Y. X. Nonstrained″ γ-Butyrolactone-Based Copolyesters: Copolymerization Characteristics and Composition-Dependent (Thermal, Eutectic, Cocrystallization, and Degradation) Properties. *Macromolecules* **2017**, *50*, 8469−8479.
(38) Hu, S.; Zhao, J.; Zhang, G.; Schlaad, H. Macromolecular Architectures through Organocatalysis. *Prog. Polym. Sci.* **2017**, *74*, 34−77.
(39) Bates, F. S.; Hillmyer, M. A.; Lodge, T. P.; Bates, C. M.; Delaney, K. T.; Fredrickson, G. H. Multiblock Polymers: Panacea or Pandora's Box? *Science* **2012**, *336*, 434−440.
(40) Ma, Y.; You, X.; Zhang, J.; Wang, X.; Kou, X.; Liu, S.; Zhong, R.; Li, Z. Synthesis of Sequence-specific Poly(ester-carbonate) Copolymers via Chemoselective Terpolymerization Controlled by the Stoichiometric Ratio of Phosphazene/Triethylborane. *Angew. Chem., Int. Ed.* **2023**, *62*, No. e202303315.
(41) Zhang, J.; Wang, L.; Liu, S.; Li, Z. Synthesis of Diverse Polycarbonates by Organocatalytic Copolymerization of CO_2 and Epoxides: From High Pressure and Temperature to Ambient Conditions. *Angew. Chem., Int. Ed.* **2022**, *61*, No. e202111197.
(42) Zhang, J.; Wang, L.; Liu, S.; Kang, X.; Li, Z. A Lewis Pair as Organocatalyst for One-Pot Synthesis of Block Copolymers from a Mixture of Epoxide, Anhydride, and CO_2. *Macromolecules* **2021**, *54*, 763−772.
(43) Ma, Y.; Wang, Z.; Jiang, L.; Zhang, J.; Ren, C.; Kou, X.; Liu, S.; Li, Z. Bulky Phosphazenium Salt Controlling Chemoselective Terpolymerization of Epoxide, Anhydride and CO_2: From Well-Defined Block to Truly Random Copolymers. *Angew. Chem., Int. Ed.* **2024**, *64*, No. e202416104.
(44) Yue, S.; Bai, T.; Xu, S.; Shen, T.; Ling, J.; Ni, X. Ring-Opening Polymerization of CO_2-Based Disubstituted delta-Valerolactone toward Sustainable Functional Polyesters. *ACS Macro Lett.* **2021**, *10*, 1055−1060.
(45) Wang, Z.; Zheng, W.; Yue, S.; Chen, K.; Ling, J.; Ni, X. Random Terpolymer of Carbon Dioxide, Butadiene and Epoxides: Synthesis, Functionalization and Degradability. *Chin. J. Chem.* **2024**, *42*, 1630−1636.
(46) Chen, K.; Zhu, Z.; Bai, T.; Mei, Y.; Shen, T.; Ling, J.; Ni, X. A Topology-Defined Polyester Elastomer from CO2 and 1,3-Butadiene: A One-Pot-One-Step "Scrambling Polymerizations" Strategy. *Angew. Chem., Int. Ed.* **2022**, *61*, No. e202213028.
(47) Zhao, Y.; Zhang, X.; Li, Z.; Li, Z.; Tang, S. Functional and Degradable Polyester-co-Polyethers from CO_2, Butadiene, and Epoxides. *ACS Macro Lett.* **2024**, *13*, 315−321.
(48) Fastnacht, K. V.; Spink, S. S.; Dharmaratne, N. U.; Pothupitiya, J. U.; Datta, P. P.; Kiesewetter, E. T.; Kiesewetter, M. K. Bis- and Tris-Urea H-Bond Donors for Ring-Opening Polymerization: Unprecedented Activity and Control from an Organocatalyst. *ACS Macro Lett.* **2016**, *5*, 982−986.
(49) Liu, Y.; Zhang, J.; Kou, X.; Liu, S.; Li, Z. Highly Active Organocatalysts for Stereoselective Ring-Opening Polymerization of Racemic Lactide at Room Temperature. *ACS Macro Lett.* **2022**, *11*, 1183−1189.
(50) Mayo, F. R.; Lewis, F. M. Copolymerization. I. A Basis for Comparing the Behavior of Monomers in Copolymerization; The Copolymerization of Styrene and Methyl Methacrylate. *J. Am. Chem. Soc.* **1944**, *66*, 1594−1601.
(51) Sathyan, A.; Hayward, R. C.; Emrick, T. Ring-Opening Polymerization of Allyl-Functionalized Lactams. *Macromolecules* **2019**, *52*, 167−175.
(52) Hoyle, C. E.; Bowman, C. N. Thiol−Ene Click Chemistry. *Angew. Chem., Int. Ed.* **2010**, *49*, 1540−1573.
(53) Becker, G.; Wurm, F. R. Functional Biodegradable Polymers via Ring-Opening Polymerization of Monomers without Protective Groups. *Chem. Soc. Rev.* **2018**, *47*, 7739−7782.
(54) Rainbolt, E. A.; Washington, K. E.; Biewer, M. C.; Stefan, M. C. Recent Developments in Micellar Drug Carriers Featuring Substituted Poly(ε-caprolactone)s. *Polym. Chem.* **2015**, *6*, 2369−2381.
(55) Pelegri-O'Day, E. M.; Paluck, S. J.; Maynard, H. D. Substituted Polyesters by Thiol−Ene Modification: Rapid Diversification for Therapeutic Protein Stabilization. *J. Am. Chem. Soc.* **2017**, *139*, 1145−1154.
(56) Liu, Z.-H.; Li, Y.; Zhang, C.-J.; Zhang, Y.-Y.; Cao, X.-H.; Zhang, X.-H. Synthesis of High-Molecular-Weight Poly(ε-caprolactone) via Heterogeneous Zinc-Cobalt(III) Double Metal Cyanide Complex. *Giant* **2020**, *3*, 100030.
(57) Grosvenor, M. P.; Staniforth, J. N. The Effect of Molecular Weight on the Rheological and Tensile Properties of Poly(ε-caprolactone). *Int. J. Pharm.* **1996**, *135*, 103−109.

https://doi.org/10.1021/acs.macromol.5c00076
Macromolecules 2025, 58, 3497−3508

(58) Fernández-Tena, A.; Pérez-Camargo, R. A.; Coulembier, O.; Sangroniz, L.; Aranburu, N.; Guerrica-Echevarria, G.; Liu, G.; Wang, D.; Cavallo, D.; Müller, A. J. Effect of Molecular Weight on the Crystallization and Melt Memory of Poly(ε-caprolactone) (PCL). *Macromolecules* **2023**, *56*, 4602−4620.
(59) Sangroniz, L.; Barbieri, F.; Cavallo, D.; Santamaria, A.; Alamo, R. G.; Müller, A. J. Rheology of Self-Nucleated Poly(ε-caprolactone) Melts. *Eur. Polym. J.* **2018**, *99*, 495−503.
(60) Ugartemendia, J. M.; Muñoz, M. E.; Sarasua, J. R.; Santamaria, A. Phase Behavior and Effects of Microstructure on Viscoelastic Properties of a Series of Polylactides and Polylactide/Poly(ε-caprolactone) Copolymers. *Rheol. Acta* **2014**, *53*, 857−868.
(61) Noroozi, N.; Thomson, J. A.; Noroozi, N.; Schafer, L. L.; Hatzikiriakos, S. G. Viscoelastic Behaviour and Flow Instabilities of Biodegradable Poly (ε-caprolactone) Polyesters. *Rheol. Acta* **2012**, *51*, 179−192.
(62) Gimenez, J.; Cassagnau, P.; Fulchiron, R.; Michel, A. Structure and Dynamics of Melt Poly(ε-caprolactone) from Inverse Rheological Calculation. *Macromol. Chem. Phys.* **2000**, *201*, 479−490.
(63) Safari, M.; Mugica, A.; Zubitur, M.; Martínez de Ilarduya, A.; Muñoz-Guerra, S.; Müller, A. J. Controlling the Isothermal Crystallization of Isodimorphic PBS-ran-PCL Random Copolymers by Varying Composition and Supercooling. *Polymers* **2019**, *12*, 17.
(64) Zhang, Z.; Quinn, E. C.; Olmedo-Martínez, J. L.; Caputo, M. R.; Franklin, K. A.; Müller, A. J.; Chen, E. Y. -. Toughening Brittle Bio-P3HB with Synthetic P3HB of Engineered Stereomicrostructures. *Angew. Chem., Int. Ed.* **2023**, *62*, No. e202311264.
(65) Zhou, L.; Zhang, Z.; Shi, C.; Scoti, M.; Barange, D. K.; Gowda, R. R.; Chen, E. Y. X. Chemically Circular, Mechanically Tough, and Melt-Processable Polyhydroxyalkanoates. *Science* **2023**, *380*, 64−69.
(66) Shen, Y.; Xiong, W.; Li, Y.; Zhao, Z.; Lu, H.; Li, Z. Chemoselective Polymerization of Fully Biorenewable α-Methylene-γ-Butyrolactone Using Organophosphazene/Urea Binary Catalysts Toward Sustainable Polyesters. *CCS Chem.* **2021**, *3*, 620−630.
(67) Zhao, N.; Ren, C.; Li, H.; Li, Y.; Liu, S.; Li, Z. Selective Ring-Opening Polymerization of Non-Strained γ-Butyrolactone Catalyzed by A Cyclic Trimeric Phosphazene Base. *Angew. Chem., Int. Ed.* **2017**, *56*, 12987−12990.

https://doi.org/10.1021/acs.macromol.5c00076
Macromolecules 2025, 58, 3497−3508